

# Influence of Bandgap Narrowing and Carrier Lifetimes on the Forward Current-Voltage Characteristics of a 4H-SiC p-i-n Diode

Gesualdo Donnarumma<sup>a,b</sup>, Vassil Palankovski<sup>a,b</sup>,  
Siegfried Selberherr<sup>b</sup>

<sup>a</sup> Advanced Materials and Device Analysis Group at the  
<sup>b</sup> Institute for Microelectronics, TU Wien,  
Gußhausstraße 27–29/E360, A-1040 Wien, Austria  
{donnarumma|palankovski|selberherr}@iue.tuwien.ac.at

Janusz Wozny<sup>c</sup>, Andrzej Kubiak<sup>c</sup>, Lukasz Ruta<sup>c</sup>,  
Zbigniew Lisik<sup>c</sup>

<sup>c</sup> Department of Semiconductor and Optoelectronic Devices,  
TU Lodz, Wolczanska 211/215, 90-924 Lodz, Poland  
{janusz.wozny|andrzej.kubiak|lukasz.ruta|  
zbigniew.lisik}@p.lodz.pl

**Abstract**—This work covers several aspects concerning SiC device modeling. The influence of the bandgap energy, bandgap narrowing, and carrier lifetimes on the forward current-voltage characteristics of a manufactured p-i-n 4H-SiC is studied. Different models are addressed and differences are shown throughout two-dimensional numerical simulations.

*Semiconductor device modeling, Silicon carbide, Device simulation*

## I. INTRODUCTION

Nowadays very intensive research on wide bandgap semiconductors is carried out. In particular SiC attracts strong attention due to its relevant and very attractive features compared to Si, such as larger bandgap, higher thermal conductivity, electron saturation velocity, and critical electric field strength [1]. These properties make SiC the foremost semiconductor material for optoelectronic, high temperature, high-power, and high-frequency electronic devices. Apart from the technological processes, device modeling has its own relevance. Many Electronic Design Automation (EDA) platforms such as multi-purpose general device simulators designed to work with fairly arbitrary semiconductor device structures are available. Moreover, several device simulators such as TCAD-Sentaurus [2], ATLAS [3], Minimos-NT [4], allow addressing various semiconductor materials, including SiC. Device simulators are available, however, the physical models and their parameters remain an issue in modeling SiC devices, which is imposed by the absence of a well-defined set of physical parameter values for the most common polytypes, e.g. 3C, 4H, and 6H, where the data available in literature scatter.

In this paper the on-state voltage dependence of a manufactured 4H-SiC p-i-n diode on bandgap energy and carrier lifetime is studied. The influence of bandgap narrowing is taken into account. Two carrier lifetime models extracted from measured data are employed in this investigation. The

impact of these models on the forward current-voltage characteristics is shown. The investigation is performed using Minimos-NT [4] and ELTER-SiC [5]. Both simulators are capable to handle SiC device simulations. Device structure, fabrication, and physical models are described in Section II and Section III, simulation results are presented in Section IV, respectively.

## II. DEVICE STRUCTURE AND FABRICATION

The investigated 4H-SiC p-i-n diode structure is shown in Fig. 1. The p<sup>+</sup> region has a doping concentration of 10<sup>20</sup>cm<sup>-3</sup>, while the epi-layer a doping of 10<sup>16</sup>cm<sup>-3</sup>, and the n<sup>-</sup> region of 10<sup>18</sup>cm<sup>-3</sup>. The device dimensions are shown in the schematic description in Fig. 1.

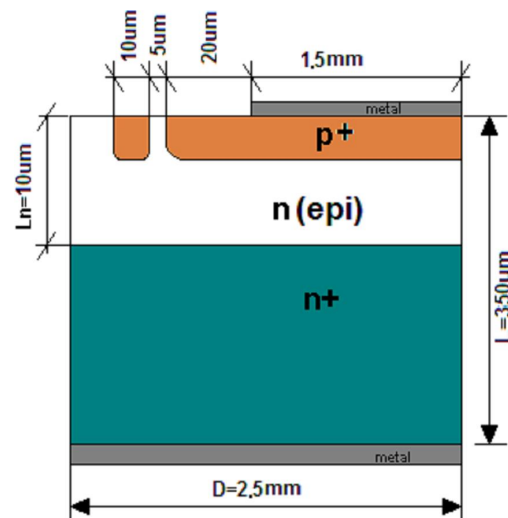


Figure 1. Investigated 4H-SiC p-i-n diode structure

This work was supported by the Austrian Science Funds FWF, START Project No. Y247-N13.

To realize the  $p^+$  region an ion implantation process is used, and a subsequent annealing process is required to electrically activate the dopant atoms. The diode was fabricated on a 3" 350 $\mu\text{m}$  thick  $n^+$  SiC wafer with 10 $\mu\text{m}$  lightly  $n$ -doped epi layer. First, the Al ion implantation process was used to create the  $p^+$  layer. A  $\text{SiO}_2$  buffer layer and PVD process for Al deposition were used to create an appropriate mask, since  $p^+$  rings were fabricated during the same ion implantation process. To achieve a proper doping profile several implantation steps with energies from 100keV to 250keV were performed. After removing the mask, the doping was activated by a 15min annealing process at 1500°C. A proper mask for the top side and PVD deposition were used to realize the Al contact on the  $p^+$  layer, and Ni for the bottom contact. A thin layer of Ni was also deposited on Al in order to avoid evaporation of the metal during annealing. To obtain Ohmic contacts a second annealing process (1000°C, 20min) was realized. Then, the diodes were cut, cleaned, and measured. More details of the device processing and characterization are given in [6].

### III. PHYSICAL MODELS

Since the area of this device structure is rather large (Fig. 1), in order to save computational effort only half of the real symmetric diode structure is simulated. The numerical analyses were performed with Minimos-NT and ELTER-SiC. The drift-diffusion transport model [7], which is suitable due to the large device dimensions, was employed in both simulators. Furthermore, all important physical models, such as Shockley-Read-Hall recombination, bandgap narrowing, and doping dependent mobility were taken into account. The measured current-voltage characteristics of the fabricated 4H-SiC  $p$ - $i$ - $n$  diode show a forward drop of 2.6V, while both two-dimensional device simulators, using the same values for the model parameters, give a forward drop of 2.8V. Fig. 2 compares our measurements and numerical simulations. Reported measurements values for the bandgap energy for 4H-SiC are typically in the range between 3.2 – 3.3eV [8], [9], [10], [11], [12], at 300K. In the literature, there are also reported values equal to 3.03eV [13] at 300K, and 3.28eV, at 4K [14]. Employing different bandgap energy values the forward current-voltage characteristic shifts. The forward drop difference between measured data and simulated curves, can be attributed either to a reduction of the bandgap energy due to bandgap narrowing or due to the carriers' lifetime. Reduction of the bandgap energy due to bandgap narrowing is taken into account considering several models. Fig. 4 shows the difference between the models of Schubert [15], Lindefelt [16], and Slotboom [17]. The first model is physics-based, where bandgap narrowing is a result of five types of many-body interactions, and is given by

$$\Delta E_g = \frac{-q^2 \beta}{4\pi\epsilon_0\epsilon_r} \quad (1)$$

$\beta$  is the inverse Thomas-Fermi length. In [16] the model for the band edge displacement and bandgap narrowing is derived for hexagonal lattices. The last model is relatively simple and is widely used for silicon.

In Fig. 4 is visible how the band edge displacement with the model of [17] is a crude approximation with respect to the other two models. Furthermore, our investigations show the possible influence of the carrier lifetime on the forward current-voltage characteristics. The carrier lifetime is one of the most important parameters of high-voltage bipolar devices. Fig. 5 shows several measured data [13], [18], [19], [20], [21], [22], [23], [24], and two distinct models Model 1, and Model 2, respectively. The carrier lifetime as function of carrier density is obtained by fitting measured data [17], [18] (Fig. 5). Several authors suggest that the carrier lifetime for low concentration should be in the range of  $\mu\text{s}$ . Different techniques, such as time-resolved photoluminescence (TRPL), microwave photoconductivity decay ( $\mu$ -PCD) are used to measure the carrier lifetime, although as shown in [24], current recovery time (CRT) technique or open circuit voltage decay (OCVD) may give incorrect results for the carrier lifetime. The decrease in carrier lifetime described by the empirical formula (2) is used in our simulations.

$$\tau = \frac{\tau_{\max}}{1 + \left(\frac{N}{N_{\text{ref}}}\right)^\gamma} \quad (2)$$

We found, the parameter set  $\tau_{\max}=240$  ns,  $N_{\text{ref}}=2 \times 10^{18} \text{cm}^{-3}$  and  $\gamma=1.9$  best match the data from [13], while the parameter set  $\tau_{\max}=12$ ns,  $N_{\text{ref}}=4 \times 10^{18} \text{cm}^{-3}$  and  $\gamma=1.4$  reproduces the data from [18]. TABLE I summarizes the values which were used in our investigation.

TABLE I. 4H-SiC PHYSICAL PARAMETERS

		<i>Model 1</i>	<i>Model 2</i>
$\tau_{\max}$	[ns]	240	12
$N_{\text{ref}}$	[ $\text{cm}^{-3}$ ]	$2 \times 10^{18}$	$4 \times 10^{18}$
$\gamma$		1.9	1.4
$E_g$	[eV]	3.23	
$\Delta E_c/\Delta E_g$		0.7	

### IV. SIMULATION RESULTS

The forward current-voltage characteristics were calculated with both simulators. The numerical results show a higher on-state voltage employing a bandgap energy value equal to 3.2eV. Fig. 2 shows the simulated I-V curves obtained with both simulators compared to the measured data. The three solid lines are obtained 1) using a bandgap energy of  $\sim 3.0\text{eV}$  (black and blue solid lines); 2) using electron and hole lifetimes of  $\tau_n=1\text{ns}$  and  $\tau_h=0.3\text{ns}$  (green line), respectively. In both investigations a bandgap narrowing model was not used. Numerical investigations presenting a forward drop of 2.8V (dashed lines), are obtained using a bandgap energy value of  $\sim 3.17\text{eV}$  in both simulators. The gap between the two forward simulated curves (black and blue dashed lines) and the measurement is about 0.2V, that is also the difference between the two bandgap energies used in the simulations.

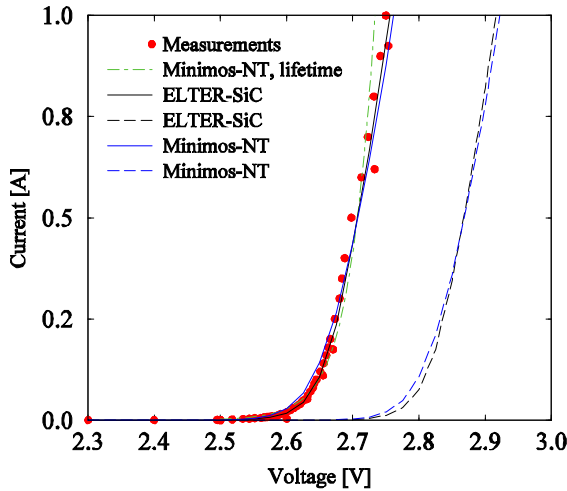


Figure 2. Comparison between measured and simulated IV curves with ELTER-SiC and Minimos-NT

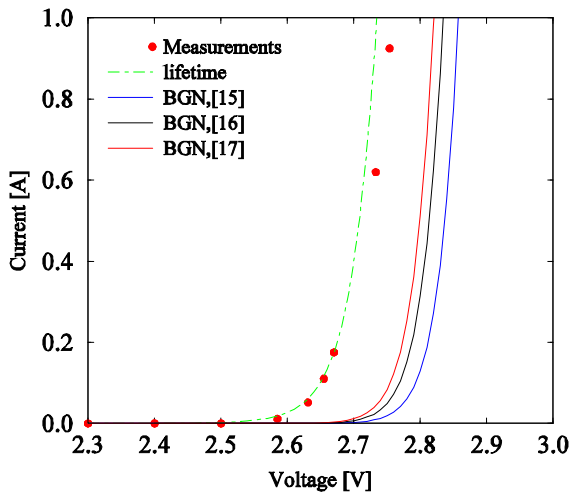


Figure 3. Bandgap narrowing influence on the simulated IV curves

A very small difference is visible between the two I-V characteristics obtained with both simulators. The forward voltage drop change due to carrier lifetime was not analyzed using ELTER-SiC. The bandgap energy reduction due to bandgap narrowing was successively included in our investigation. The bandgap energy value used was 3.2eV. Three different models were employed (Fig. 4). Simulations employing only bandgap narrowing reduce the forward voltage drop to about 2.8V, although this effect appears to be highly relevant, the carrier lifetime is still prominent. The bandgap narrowing model based on [16] provides similar results as that from [15]. Fig. 3 shows the bandgap narrowing influence on the simulated I-V curves, together with the carrier lifetime. In the literature the lowest reported carrier lifetimes measured for 4H-SiC range between ~20ns [15] and ~2ns [16] (Fig. 3).

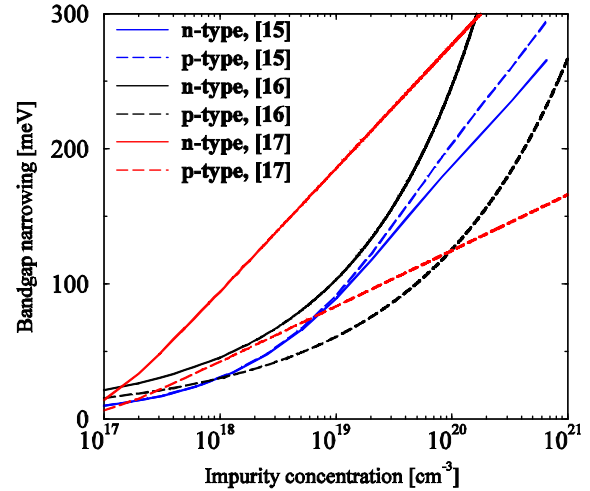


Figure 4. Comparison of bandgap narrowing models

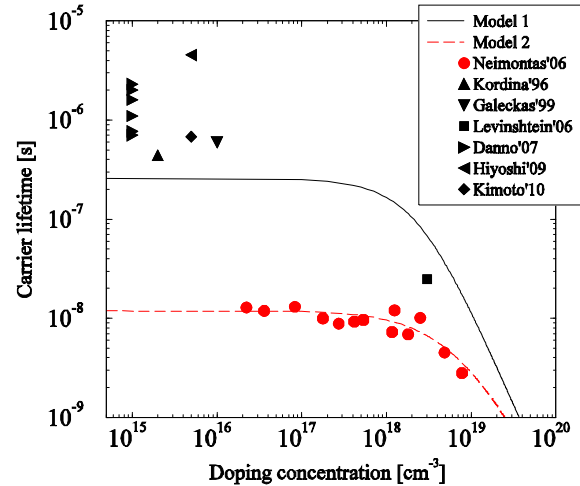


Figure 5. Carrier lifetime as a function of doping concentration: experimental data (symbols) and models (lines)

Since in the first investigation (Fig.2) the carrier lifetime values used for the best fit are much smaller than any reported measured data, both bandgap narrowing and carrier lifetime modeling must be used in order to address the on-state voltage shift. Two distinct carrier lifetime models which fit the measured data [13], [18] have been evaluated. Fig. 5 shows experimental data (symbols) and models (lines). The first model is derived in order to approximate the highest values of the carrier lifetimes  $\tau_{max}$  for low doping concentration. The second model instead is fitted to give better agreement with the lowest values for high doping concentration, reducing more the on-state forward voltage gap from the measured data. Employing Model 2 the on-state voltage is reduced more in respect to Model 1, as expected. Numerical results show (Fig. 6) the forward current-voltage characteristics change due to the

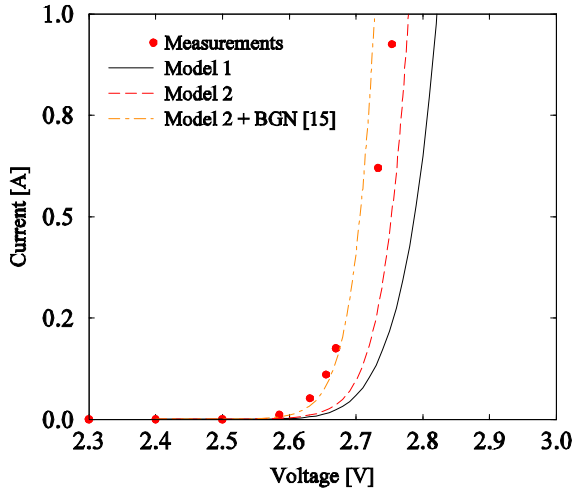


Figure 6. Bandgap narrowing and carrier lifetime influence on the simulated IV curves

carrier lifetime using Model 1 and Model 2, respectively. To obtain a closer agreement with the measured data, we took into account also the bandgap narrowing model (1), together with Model 2. The bandgap narrowing contribution to the conduction band  $\Delta E_c/\Delta E_g = 0.7$  is chosen. Results are shown in Fig. 6. Although the simplest model [17] reduce the forward drop significantly, as seen in Fig.3, a more sophisticated model, e.g., the Schubert or Lindefelt model, should be preferred. Moreover, in our investigation self-heating was taken into account, however, only a negligible influence on the forward current voltage characteristics was observed. The bandgap energy value for 4H-SiC may be set to 3.2eV (at 300 K), however carrier lifetime and bandgap narrowing play an important role, and must be addressed consistently in SiC device modeling.

## V. RESULTS

We present results from two-dimensional physical-based numerical simulations of 4H-SiC p-i-n diodes using ELTER-SiC and Minimos-NT. Our investigations show the influence of the bandgap energy and carrier lifetimes on the on-state resistance. Simulation results using different models and parameter values were compared to measured data.

## REFERENCES

- [1] W. J. Choyke, H. Matsunami, G. Pensl, *Silicon Carbide: Recent Major Advances*, Springer, New York, 2004.
- [2] Synopsys, *Sentaurus Device User Guide, Version A-2008.09*, 2008.
- [3] Silvaco International, *ATLAS User's Manual, ed. 6, Santa Clara*, 1998.
- [4] T. Binder, K. Dragosits, T. Grasser, R. Klima, M. Knaipp, H. Kosina, R. Mlekus, V. Palankovski, M. Rottinger, G. Schrom, S. Selberherr, and M.

- Stockinger, *MINIMOS-NT User's Guide*. Institut für Mikroelektronik, Technische Universität Wien, 1998.
- [5] G. Donnarumma, "Modelling of Electric Phenomena in Anisotropic Semiconductor Structures," Ph.D. dissertation, TU Lodz, 2011.
- [6] A. Kubiak, Z. Lisik, A. Kalinowski, L. Ruta, "Silicon carbide p-i-n diode," in *Proc. MICROTHERM'11 Conf.*, pp. 179-184, 2011.
- [7] S. Selberherr, *Analysis and Simulation of Semiconductor Devices*, Springer, Wien, 1984.
- [8] M.E. Levinshtein, S.L. Rumyantsev, M.S. Shur, *Properties of Advanced Semiconductor Materials*, Wiley, New York, 2001.
- [9] C. Persson, U. Lindefelt, "Relativistic band structure calculation of cubic and hexagonal SiC polytypes," *J. Appl. Phys.*, vol. 82, pp. 5496-5508, 1997.
- [10] K. Bertilsson, "Simulation and Optimization of SiC Field Effect Transistors," Dissertation, KTH Microelectronics and Information Technology, Stockholm, 2004.
- [11] K. Takahashi, A. Yoshikawa and A. Sandhu, *Wide Bandgap Semiconductors*, Springer, New York, 2007.
- [12] G.L. Harris, *Properties of Silicon Carbide*, INSPEC, London, 1995.
- [13] A. Galeckas, J. Linnros, V. Grivickas, U. Lindefelt, and C.Hallin, "Evaluation of Auger recombination rate in 4H-SiC," Proceedings of the 7th International Conference on SiC, III-Nitrides and Related Materials, Aug.31-Sept.5, 1997, Stockholm, Sweden 1997, pp.533-536.
- [14] S. Sandeep, R. Komaragiri, "Simulation and comparison studies of silicon carbide and silicon power devices," in *Proc. IICPE Conf.*, pp.1-5, 2010.
- [15] E. Schubert, *Doping in III-V Semiconductors*, Cambridge University Press, 2005.
- [16] U. Lindefelt, "Doping-induced band edge displacements and bandgap narrowing in 3C-, 4H-, 6H-SiC, and Si," *J. Appl. Phys.*, vol. 84, pp. 2628-2637, 1998.
- [17] J. W. Slotboom and H. C. DeGraff, "Measurement of bandgap narrowing in silicon bipolar transistors," *Solid-State Electron.*, vol. 19, pp. 857-862, 1976.
- [18] K. Neimontas, T. Malinauskas, R. Aleksejunas, M. Sudzius, K. Jarasiunas, J. Storasta, P. Bergman and E. Janzen, "The determination of high-density carrier plasma parameters in epitaxial layers, semi-insulating and heavily doped crystals of 4H-SiC by a picosecond four-wave mixing technique," *Semicond. Sci. Technol.* vol. 21, pp. 952-958, 2006.
- [19] T. Kimoto, Y. Nanen, T. Hayashi, and J. Suda, "Enhancement of carrier lifetimes in n-Type 4H-SiC epitaxial layers by improved surface passivation," *Appl. Phys. Express* 3, pp. 1-3, 2010.
- [20] O. Kordina, J. P. Bergman, C. Hallin, and E. Janzen, "The minority carrier lifetime on n-type 4H- and 6H-SiC epitaxial layers," *Appl. Phys. Lett.*, vol. 69, pp. 679-681, 1996.
- [21] A. Galeckas, J. Linnros, M. Frischholz, K. Rottner, N. Nordell, S. Karlsson, V. Grivickas, "Investigation of surface recombination and carrier lifetime in 4H/6H-SiC," *Material Science and Engineering B*, vols. 61-62, pp. 239-243, 1999.
- [22] T. Hiyoshi, and T. Kimoto, "Elimination of the major deep levels in n- and p-type 4H-SiC by two-step thermal treatment," *Appl. Phys. Express* 2, pp. 1-3, 2009.
- [23] K. Danno, D. Nakamura, T. Kimoto, "Investigation of carrier lifetime in 4H-SiC epilayers and lifetime control by electron irradiation," *Appl. Phys. Lett.*, vol. 90, pp. 1-3, 2007.
- [24] M. E. Levinshtein, T. T. Mnatsakanov, P. Ivanov, J. W. Palmour, S. L. Rumyantsev, R. Singh, and S. N. Yurkov, "Paradoxes of carrier lifetime measurements in high-voltage SiC diodes," *IEEE Trans. Electron. Devices*, vol.48, no. 8, pp. 1703-1710, 2001.